Mathematical Biosciences 365 (2023) 109075

Contents lists available at ScienceDirect

Mathematical Biosciences

journal homepage: www.elsevier.com/locate/mbs

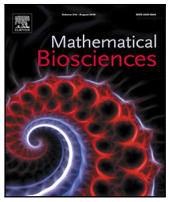

Original Research Article

Variation in environmental stochasticity dramatically affects viability and extinction time in a predator–prey system with high prey group cohesion

Tao Feng [a], Russell Milne [b], Hao Wang [b,*]

[a] School of Mathematical Science, Yangzhou University, Yangzhou, Jiangsu 225002, PR China
[b] Department of Mathematical and Statistical Sciences & Interdisciplinary Lab for Mathematical Ecology and Epidemiology, University of Alberta, Edmonton, AB T6G 2G1, Canada

ARTICLE INFO

Keywords:
Predator–prey model
Noise-induced tipping
Allee effect
Holling type IV functional response

ABSTRACT

Understanding how tipping points arise is critical for population protection and ecosystem robustness. This work evaluates the impact of environmental stochasticity on the emergence of tipping points in a predator–prey system subject to the Allee effect and Holling type IV functional response, modeling an environment in which the prey has high group cohesion. We analyze the relationship between stochasticity and the probability and time that predator and prey populations in our model tip between different steady states. We evaluate the safety from extinction of different population values for each species, and accordingly assign extinction warning levels to these population values. Our analysis suggests that the effects of environmental stochasticity on tipping phenomena are scenario-dependent but follow a few interpretable trends. The probability of tipping towards a steady state in which one or both species go extinct generally monotonically increased with noise intensity, while the probability of tipping towards a more favorable steady state (in which more species were viable) usually peaked at intermediate noise intensity. For tipping between two equilibria where a given species was at risk of extinction in one equilibrium but not the other, noise affecting that species had greater impact on tipping probability than noise affecting the other species. Noise in the predator population facilitated quicker tipping to extinction equilibria, whereas prey noise instead often slowed down extinction. Changes in warning level for initial population values due to noise were most apparent near attraction basin boundaries, but noise of sufficient magnitude (especially in the predator population) could alter risk even far away from these boundaries. Our model provides critical theoretical insights for the conservation of population diversity: management criteria and early warning signals can be developed based on our results to keep populations away from destructive critical thresholds.

1. Introduction

Recently, ecological tipping points, where the state of an ecosystem abruptly transitions from a steady state to an alternate dynamic regime, have been increasingly observed in the field [1,2]. It is known that the emergence of these tipping points can disrupt interactions between prey and predator populations, and therefore potentially lead to the collapse of important ecosystem functions [3]. Hence, much contemporary research has focused on identifying and preparing for these ecological transitions, including finding early warning signals before catastrophic thresholds are approached (see e.g. [4]). This has incorporated both experimental and theoretical work, and has led to advances that link both of these domains, such as inferring bifurcations in population data that are directly due to manipulation of environmental parameters in a lab setting [4,5], refining tipping point detection methodology to reduce false positives [6], and mathematical derivation of control methods and management strategies for ecosystems vulnerable to tipping [7,8]. The study of tipping points has additionally been extended to those taking place over larger spatial scales, by the use of network-based models [9–11]. Because of the possibility for sudden and potentially irreversible changes to an ecosystem that tipping brings with it, understanding the mechanisms by which tipping points occur is crucial for population conservation.

Within ecology, tipping points are classically categorized based on what causes them. Bifurcation-induced tipping occurs when changes in an environmental parameter cause it to pass through a critical threshold, at which point a previously stable steady state destabilizes or disappears [12–15]. Rate-induced tipping occurs when an environmental parameter changes too quickly. This changes the locations of the system's equilibria, as well as the boundaries of their basins of

* Corresponding author.
E-mail addresses: tfeng.math@gmail.com (T. Feng), rmilne@ualberta.ca (R. Milne), hao8@ualberta.ca (H. Wang).

https://doi.org/10.1016/j.mbs.2023.109075
Received 31 January 2023; Received in revised form 13 August 2023; Accepted 6 September 2023
Available online 19 September 2023

attraction, making the system fail to track a continuously changing attractor and move into a different attraction basin [1,16–18]. Noise-induced tipping happens when environmental stochasticity drives the system too far from the steady state, leading it on a path that instead draws it towards a different one [19–21]. Phase tipping occurs when external input causes the system to tip to a different steady state due to stochastic noise or rapid parameter changes, but only for certain areas of a given steady state's neighborhood, commonly expressed as phase values of a periodic orbit [22,23].

Most fluctuations in species' populations can be attributed to environmental stochasticity rather than periodic or chaotic phenomena, and environmental stochasticity has been shown to lead to the irreversible collapse of populations from persistence to extinction [24]. Because of this, noise-induced tipping is likely to have outsize effects on predator–prey interactions. So far, theoretical studies on how environmental stochasticity affects steady-state switching have yielded important insights. For example, Meng et al. [25] explored the effect of stochasticity on average transient time in complex mutualistic networks of plant and pollinator species, finding that increases in the amplitude of the system's noise terms result in shorter transient times, with an algebraic relationship between the two conjectured. Similarly, prior work on stochasticity and tipping within a model of glycolysis showed that noise can induce rich dynamical behavior even within a relatively simple framework [26], indicating that the appearance of similarly complex phenomena in a stochastic predator–prey model is likely. At the same time, few studies have explored the relationship between environmental stochasticity and the probability and time of tipping point occurrence, as well as the problem of identifying which predator and prey population levels produce heightened extinction risk in stochastic environments.

Predator–prey interaction is the primary driving force for energy transfer in a food web, and hence different patterns of predator–prey interaction can have broad-ranging effects throughout an ecosystem [27,28]. This means that predator–prey interaction has a profound impact on the healthy and sustainable development of ecosystems, and hence it has been a focal point for the development and testing of ecological theory (see e.g. [29,30]). Since the pioneering work of Lotka [31] and Volterra [32], researchers worldwide have explored many different aspects of the predator–prey relationship. These include prey defense against predators [33,34], delays corresponding to the predator's gestation time [35], availability of additional food sources for the predator [36], harvesting of the prey independently from predation [37], and migration patterns of both species [38], as well as extensions to specific ecosystems such as herbivorous fish grazing on algae [39] and plankton communities [40]. Due to the multitude of different ecological factors that can affect either species in a predator–prey system, intrinsic environmental fluctuations may be stronger in the population of one or the other. For instance, a disease carried only by the predators (see e.g. [41]) would have intrinsic effects on dynamics of the predators but not those of the prey. Since imbalances in predator–prey interactions can have cascading effects throughout an entire food web, stochastic variation in the population of one or the other can have significant consequences for all species within a community. Determining which of these is more likely to result in tipping will allow ecosystem managers to focus on maintaining a stable environment for whichever species is most important.

Evidence of the Allee effect has been found to be widespread in nature [42–44], with examples found in populations of both animals [45,46] and plants [47,48]. The precursors leading to the Allee effect are diverse, including ecological mechanisms such as mate limitation [49,50] and habitat alteration [43]; invasive species also often display Allee effects due to the fragmented nature of their spread into a new habitat [48,51]. Allee effects can also be caused by human-induced factors such as the overharvesting of uncommon species due to humans putting a premium on rarity [52], as well as genetic mechanisms such as inbreeding depression [53]. Because of its real-world prominence, the Allee effect has been featured in many theoretical studies in population biology (see e.g. [54–59]).

The Holling type IV functional response describes the rate of predation for a scenario in which the prey population exhibits group defense against predators, reducing predation pressure when high levels of prey are present [60–63]. This makes it conceptually similar to the Allee effect, since both represent processes with maximum efficiency at intermediate input levels. Examples of the Holling type IV functional response observed in the field include moose intimidating wolves to reduce their predation ability [64] and ant colonies acting in unison against spider attacks [65]; it can also occur in producer–grazer systems, where thick grass can inhibit grazers' mobility [66]. This formulation is capable of rich and complex dynamics: for instance, introducing group defense can cause a predator–prey system to exhibit the paradox of enrichment [67,68], but stronger levels of group defense can instead rescue a predator population from extinction [69]. Cooperation in hunting and defense against predators has been mentioned as a potential cause of the Allee effect [45], providing a link between it and the Holling Type IV functional response. Consequently, a predator–prey system in which the prey has a high level of group cohesion would be expected to exhibit both of these phenomena. However, studies on the vulnerability to tipping of a predator–prey system featuring both of these mechanisms have not yet been conducted, despite their fundamental importance in ecological theory. Because demographic stochasticity can play a role in establishing Allee effects [50], determining the propensity for such systems to undergo noise-related tipping is especially important.

The rest of the paper is organized as follows. Section 2 illustrates the derivation of the stochastic predator–prey system and the techniques used to obtain the main results. Section 3 presents the main results of the paper. Section 4 concludes the work with a summary of results, and potential future work.

2. Methods and model formulation

2.1. Model formulation

A general predator–prey system can be described by the following differential equation model [70]

$$\begin{cases} \dfrac{\mathrm{d}x}{\mathrm{d}t} = q(x)x - p(x)y, \\ \dfrac{\mathrm{d}y}{\mathrm{d}t} = cp(x)y - dy, \end{cases} \tag{1}$$

where $x(t)$ and $y(t)$ represent the density of prey and predator populations at time t, respectively. Prey grow at a rate $q(x)$ and are eaten by predators at a rate $p(x)$, which can vary between models, while c represents the conversion rate of prey into predators and d is the predator death rate. In this work, we will consider the case where the growth rate of the prey population is affected by the Allee effect, and the predator population obeys the Holling type IV functional response. Taking the general model (1) as the starting point, the derivation of the predator–prey model with the Allee effect and a Holling type IV functional response is presented below.

The Allee effect was first discovered by Warder Clyde Allee in an experiment on the survival rate of goldfish in the 1930s; it describes a positive association between the per-individual growth rate and population density [71]. At the scale level, there can exist the component Allee effect (i.e., the positive relationship between any measurable component of individual fitness and population density) and the demographic Allee effect (i.e., the positive relationship between overall individual fitness and population density). According to the nature of density dependence at low densities, the demographic Allee effect can be divided into two types: the strong Allee effect and the weak Allee effect (see Fig. B.1), where the strong Allee effect results in a critical population density under which the population growth rate becomes negative [43].

To incorporate the Allee effect, we assume that the density-dependent growth rate $q(x)$ takes the form

$$q(x) = r(K - x)(x - A),$$

where r is the intrinsic growth rate of the prey population, K denotes the carrying capacity of the prey population in the absence of predator pressure, and A denotes the Allee threshold. In this formulation, there are three distinct cases for the nature of the Allee effect, depending on the value of A. Firstly, when $K > A > 0$, the strong Allee effect emerges, i.e. prey population growth is negative when $x < A$. Secondly, when $-K < A < 0$, the weak Allee effect emerges, where low values of x mean lower, but not negative, prey growth. Lastly, when $A = 0$, the Allee effect disappears.

The functional response describes the relationship between the amount of prey consumed by a predator per unit of time and its prey density [72,73]. Classical functional responses include three introduced by Crawford Stanley (Buzz) Holling, namely Holling type I, II, and III functional responses [74]. In these three functional responses, the consumption rate of the predator increases monotonically with prey density, and saturates when prey density is large enough (see Fig. B.2(a) – Fig. B.2(c)). In addition to the three classic functional responses mentioned above, Holling [75] proposed a functional response with swarming effects, often referred to as Holling type IV functional response. A significant difference from the first three functional responses is that Holling type IV functional response is non-monotonic, suggesting that the consumption rate of the predator will decrease when the prey population is sufficiently dense (see Fig. B.2(d)).

To incorporate the Holling type IV functional response, we assume that

$$p(x) = \frac{mx}{ax^2 + bx + 1},$$

where $a, m > 0$, and $b > -2\sqrt{a}$ so that $p(x) > 0$ for all $x > 0$. Therefore, the predator–prey model with Allee effect and Holling type IV functional response can be shown as

$$\begin{cases} \dfrac{\mathrm{d}x}{\mathrm{d}t} = rx(K - x)(x - A) - \dfrac{mxy}{ax^2 + bx + 1}, \\ \dfrac{\mathrm{d}y}{\mathrm{d}t} = \dfrac{cmxy}{ax^2 + bx + 1} - dy. \end{cases} \tag{2}$$

Through simple calculations and referring to Arsie et al. [76], we can get the following results concerning the existence and stability of equilibria of the deterministic model (2).

Lemma 2.1. *The deterministic system (2) always has two boundary equilibria: $E_0 = (0, 0)$ representing the extinction of both species and $E_K = (K, 0)$ representing the extinction of predator population; there is a third boundary equilibrium $E_A = (A, 0)$ if $0 < A < K$. Moreover, the system (2) can have up to two interior equilibria $E_1^* = (x_1^*, G(x_1^*))$ and $E_2^* = (x_2^*, G(x_2^*))$ if $d \in \left(0, \frac{cm}{2\sqrt{a}+b}\right)$, where*

$$x_1^* = \frac{cm - bd - \sqrt{(bd - cm)^2 - 4ad^2}}{2ad}, \quad x_2^* = \frac{cm - bd + \sqrt{(bd - cm)^2 - 4ad^2}}{2ad},$$

and

$$G(x_i^*) = \frac{r}{m}(K - x_i^*)(x_i^* - A)(ax_i^{*2} + bx_i^* + 1).$$

The conditions for the existence and stability of the equilibria are summarized in Table 1.

Interactions between predator and prey populations can be influenced by abiotic factors present in the surrounding environment. This includes common environmental factors such as temperature, humidity and rainfall, as well as sudden environmental factors such as volcanic eruptions and flash floods. Mathematically, common environmental factors are usually characterized by white Gaussian noise [77], while sudden environmental factors are usually described by Lévy noise [78]. In this work, we only consider the case where the predator–prey system (2) is affected by common environmental factors, and the intensity of environmental factors is positively correlated with the population density. This latter condition has been used in previous stochastic ecological systems [79], and stems from assumptions made about the format of the solution to such systems. By standard arguments [79,80], for any initial value $X_0 = (x(0), y(0))'$ and $0 \le \Delta t \ll 1$, we assume that the solution $X_t = (x(t), y(t))'$ is a Markov process with the conditional mean

$$\mathbb{E}[X_{t+\Delta t} - X_t | X = X_0] \approx \begin{bmatrix} rx(K - x)(x - A) - \frac{mxy}{ax^2+bx+1} \\ \frac{cmxy}{ax^2+bx+1} - dy \end{bmatrix} \Delta t$$

and the conditional variance

$$\mathrm{Var}[X_{t+\Delta t} - X_t | X = X_0] \approx \begin{bmatrix} \sigma_1^2 x^2 \\ \sigma_2^2 y^2 \end{bmatrix} \Delta t.$$

More formally, we can extend the deterministic model (2) to the following stochastically forced system

$$\begin{cases} \mathrm{d}x = \left[rx(K - x)(x - A) - \dfrac{mxy}{ax^2 + bx + 1}\right] \mathrm{d}t + \sigma_1 x \mathrm{d}\xi_1(t), \\ \mathrm{d}y = y\left(\dfrac{cmx}{ax^2 + bx + 1} - d\right) \mathrm{d}t + \sigma_2 y \mathrm{d}\xi_2(t), \end{cases} \tag{3}$$

where $\xi_1(t), \xi_2(t)$ are one-dimensional independent Brownian motion with intensities σ_1^2, σ_2^2, respectively. Throughout this paper, we assume that $\xi_i(t)$ are defined on the complete probability space $(\Omega, \mathcal{F}, \mathbb{P})$ with filtration $\{\mathcal{F}_t\}_{t\ge 0}$ satisfying the usual conditions.

Since System (3) describes the interactions between predator and prey populations, we need to verify that System (3) is biologically well-defined. This is done by proving that System (3) has a unique positive solution for any given initial condition, which is accomplished in Appendix A.

2.2. Methods

Here, we explain how stochastic model (3) is discretized to perform numerical simulations. We also explain how vital indicators such as the probability of and time to extinction, as well as which initial conditions are safe from extinction, are estimated.

Definition 2.1. Consider the noise-induced system

$$\mathrm{d}X(t) = \mathbf{F}(X)\mathrm{d}t + \sum_{m=1}^{k} \mathbf{G}_m(X)\mathrm{d}\xi_m(t), \tag{4}$$

and the corresponding truncated system (i.e., with $\mathbf{G}_m(X) = 0$), where $\mathbf{F}, \mathbf{G_m}, \in \mathbb{R}^n$, $\xi_m(t)$ is a standard n-dimensional independent Brownian motion. Assume that the truncated system has n ($n \ge 2$) steady states E_i, $i = 1, 2, \ldots, n$ (e.g., stable equilibria or stable cycles). When a solution starts from the basin of attraction of steady state E_1, we call the probability that the solution crosses the separatrix and settles within the basin of attraction of steady state E_j within a predetermined time interval T as the tipping probability of the solution from the steady state E_i to the steady state E_j. In addition, the time consumed by the whole tipping process is called a tipping time.

Discretization of the stochastic model (3). In order to perform numerical simulations on the stochastic predator–prey model (3), we first discretize it in time, which allows us to produce the populations in the model at a given time step as a function of the populations at the previous time step and the stochastic noise input. By using the Euler–Maruyama numerical method [81], we discretized the model as

$$\begin{aligned} \phi_{k+1} =& \phi_k + f(\phi_k)\Delta t + g(\phi_k)\xi_k\sqrt{(\Delta t)} \\ &+ \frac{1}{2}\sqrt{\Delta t}(\xi_k^2 - 1)(g(\phi_k + \sqrt{\Delta t}g(\phi_k)) - g(\phi_k)). \end{aligned} \tag{5}$$

Table 1
Existence and stability of equilibria of system (2), where DNE means that the equilibrium does not exist.

Conditions	E_0	E_A	E_K	E_1^*	E_2^*
$x_1^* < A < K < x_2^*$	stable node	unstable node	saddle	DNE	DNE
$x_1^* < x_2^* < A < K$	stable node	saddle	stable node	DNE	DNE
$A < K < x_1^* < x_2^*$	stable node	saddle	stable node	DNE	DNE
$x_1^* < A < x_2^* < K$	stable node	unstable node	stable node	DNE	saddle
$A < x_1^* < K < x_2^*$	stable node	saddle	saddle	attracting if $G'(x_1^*) < 0$ repelling if $G'(x_1^*) > 0$	DNE
$A < x_1^* < x_2^* < K$	stable node	saddle	stable node	attracting if $G'(x_1^*) < 0$ repelling if $G'(x_1^*) > 0$	saddle
$A < 0,\ K < x_1^* < x_2^*$	saddle	DNE	stable node	DNE	DNE
$A < 0,\ x_1^* < K < x_2^*$	saddle	DNE	saddle	attracting if $G'(x_1^*) < 0$ repelling if $G'(x_1^*) > 0$	DNE
$A < 0,\ x_1^* < x_2^* < K$	saddle	DNE	stable node	attracting if $G'(x_1^*) < 0$ repelling if $G'(x_1^*) > 0$	saddle

In these discretized equations, $\phi_k = (x(k), y(k))'$ is a vector containing the predator and prey populations at time k; $\Delta t = 10^{-5}$ is the time step; ξ_k for $k = 1, 2$ obey the Gaussian distribution $N(0, 1)$; and the vector-valued functions $f, g : \mathbb{R}_+^2 \to \mathbb{R}^2$ are given by

$$f(u) = \begin{bmatrix} ru_1(K - u_1)(u_1 - A) - \frac{mu_1u_2}{au_1^2 + bu_1 + 1} \\ \frac{cmu_1u_2}{au_1^2 + bu_1 + 1} - du_2 \end{bmatrix}, \quad g(u) = \begin{bmatrix} \sigma_1 u_1 \\ \sigma_2 u_2 \end{bmatrix}.$$

for an input vector $u = (u_1, u_2)' \in \mathbb{R}_+^2$.

Estimation of tipping probability. MATLAB R2021a software was employed to perform numerical simulations of the discretized system (5) on the time interval $[0, T]$, where T is set large enough to capture end behavior of the model. To determine whether a tipping point occurs, we numerically checked whether the simulated solution of the discretized system (5) falls within a small neighborhood of a given alternative steady state (i.e. besides the steady state whose basin of attraction the system was initialized in) during the interval $[0, T]$; an example of this is the neighborhood $[0, 10^{-6}]$ of the boundary equilibrium E_0 for solutions that start outside E_0's basin of attraction. If this process is performed M times (for sufficiently large M, such as $M = 10^5$), and a tipping point is present in n of these simulations, then the probability of a tipping point occurring can be estimated by the following frequency formula:

$$\mathbb{P}_{Tipping} = \frac{n}{M}.$$

Estimation of tipping time. When we performed our simulations, the probability of tipping approached 1 under some conditions. In these cases, we determined the estimated time until the system was expected to reach a tipping point. To do this, we first ran the discretized system (5) a total of $M = 10^5$ times until the tipping point appeared. During each run, we recorded the time $t_i, i = 1, 2, \ldots, M$ of the tipping point reached during that run. Therefore, the estimated tipping time can be estimated as

$$\frac{1}{M}\sum_{i=1}^{M} t_i.$$

Determination of safe areas. We also evaluated the risk of extinction associated with different initial conditions of the model, and consequently determined which initial conditions were generally safe from extinction for different levels of environmental stochasticity. To identify the extinction risk of different initial conditions, we traversed the initial population values within the space $(x(0), y(0)) \in [0, x_{\max}] \times [0, Y_{\max}]$. For each chosen initial condition, we performed the steps listed above in Definition 2.1, specifically evaluating the probability of tipping to an extinction equilibrium. After determining this probability for all surveyed initial conditions, we categorized them into four levels of extinction risk based on ranges of values that their tipping probabilities fell into, with the lowest probability range (0 to 20 percent chance of tipping to an extinction equilibrium) being designated as safe. We additionally color-coded each level of extinction risk for easy graphical interpretation: from high to low, we designated our risk levels as red, orange, yellow and blue. (Further details are available in Section 3.2.)

Table 2
Parameters for the numerical simulations of the stochastic system (3).

Parameters	Scenario 1	Scenario 2	Scenario 3	Scenario 4	Source
K	30	21	21	20	Arsie et al. [76]
A	15	−1	1	2	Arsie et al. [76]
a	0.004905	0.004905	0.004905	0.004905	Arsie et al. [76]
b	−0.10891	−0.10891	−0.10891	−0.10891	Arsie et al. [76]
c	1	1	1	1	Arsie et al. [76]
d	24.28	24.28	24.28	24.28	Arsie et al. [76]
m	1	1	1	1	Arsie et al. [76]
r	1	1	1	1	Arsie et al. [76]
σ_1	–	–	–	–	–
σ_2	–	–	–	–	–

3. Main results

Here, we evaluate the impact of environmental stochasticity on population dynamics by analyzing the relationship between vital indicators outlined previously (extinction probability, extinction time, and safe area from extinction) and the density of environmental stochasticity (hereinafter referred to as noise).

3.1. Tipping probability and tipping time

Using the numerical methods described previously, we analyze the effects of environmental stochasticity from prey and predator populations on the probability that a tipping point occurs and, when this probability is 1, the expected time until tipping. The equilibria that our system can possess, and hence can tip between, were previously established by Lemma 2.1. To ensure that our analysis is performed on a representative selection of model behavior, we use four different parameter sets that each cause the system to admit a different combination of equilibria. These parameter values are shown in Table 2.

Scenario 1. Noise-induced tipping between boundary equilibria E_0 and E_K

When $K = 30, A = 15, a = 0.004905, b = -0.10891, c = 1, d = 24.28, m = 1$, and $r = 1$, from Lemma 2.1 we know that the deterministic model (2) has four equilibria: the boundary equilibria E_0 and E_K, the Allee equilibrium E_A and the interior equilibrium E_2^*. In this case, the deterministic model (2) has bistability between the boundary equilibria E_0 and E_K, while the Allee equilibrium E_A is an unstable node and the interior equilibrium E_2^* is a saddle (see Fig. B.3). Due to the included noise, the stochastic model (3) can converge to either of the two stable equilibria from the same initial conditions (see Fig. B.4).

Fig. 1 shows that the occurrence probability of tipping points (i.e. tipping probability) is closely related to the intensity and source of noise. However, different trends were observed depending on whether the system started in the basin of attraction of E_K or that of E_0, as well as which populations (prey and/or predator) experienced noise. Because both stable equilibria in this scenario featured zero predators,

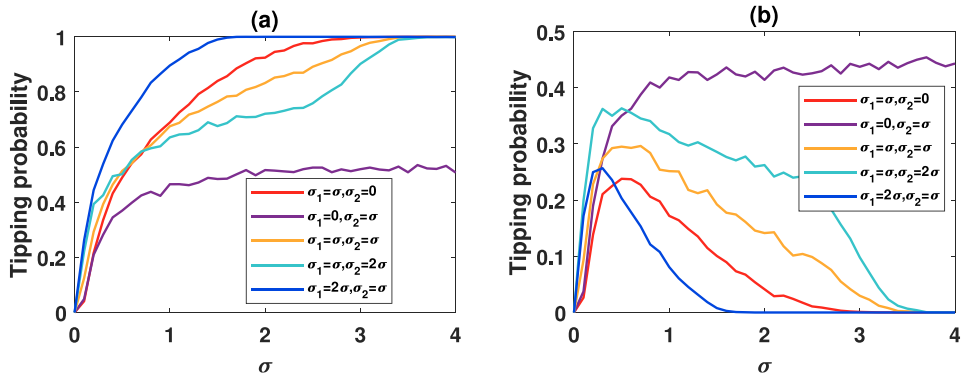

Fig. 1. Tipping probabilities of the stochastic system (3) with $K = 30, A = 15, a = 0.004905, b = -0.10891, c = 1, d = 24.28, m = 1, r = 1$. The initial values in Figs. 1(a) and 1(b) are given by $(x(0), y(0)) = (30, 80)$ (in the basin of attraction of E_K) and $(x(0), y(0)) = (30, 83)$ (in the basin of attraction of E_0), respectively.

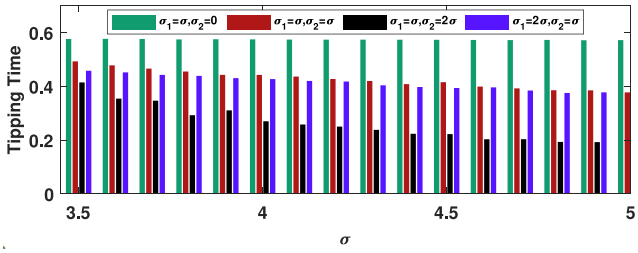

Fig. 2. Tipping times of the stochastic system (3) with $K = 30, A = 15, a = 0.004905, b = -0.10891, c = 1, d = 24.28, m = 1, r = 1$. The initial value is given by $(x(0), y(0)) = (30, 80)$, which is in the basin of attraction of E_K.

the probability of tipping depended mostly on the magnitude of noise in the prey population. When the prey population experienced noise, increasing the magnitude of this noise resulted in a monotonic increase in the likelihood of a solution starting in the basin of attraction of E_K experiencing a tipping point and being drawn instead to E_0; this probability reached 1 for sufficiently large values of prey noise intensity σ_1 (Fig. 1(a)). In contrast, for solutions starting within the basin of attraction of E_0 with prey noise present, tipping probability had a concave relationship with noise intensity: increases in σ_1 caused tipping probability first to rise and then to lower (Fig. 1(b)). This can be interpreted as small amounts of noise helping the prey escape the extinction equilibrium, but large amounts of noise preventing such an escape. If noise was present in the predator population, but not the prey, tipping probability increased with the predator noise intensity σ_2 at low levels, but saturated between 40% and 50% probability of tipping when σ_2 was increased further. This effect was nearly identical regardless of which basin of attraction the initial population densities were located in. Despite long-term predator trajectories tending towards extinction, adding noise to the predator population reduced the chances of tipping from E_K to E_0 and increased the chances of tipping in the other direction, on the whole positively affecting the prey's chances for survival. This suggests that in situations where a predator species in search of prey enters an area where it cannot survive in the long term, stochasticity affecting just the predators can still increase the likelihood of prey persistence.

Because high levels of prey noise intensity can lead to tipping from the basin of attraction of E_K to that of E_0 with probability 1, we further analyzed the tipping time in such cases. There, as with tipping probability, noise in the predator population can significantly alter tipping time despite all predator trajectories being destined for extinction (Fig. 2). When only the prey population exhibited noise, changing the intensity σ_1 of this noise had very little effect on tipping time, but additionally including nonzero noise in the predator population established a clear relationship where increasing the prey noise σ_1 and the predator noise σ_2 caused faster tipping. This relationship was mostly dependent on the predator noise. Compared to the tipping times observed when σ_1 and σ_2 were both set equal to a common value of σ, increasing the predator noise to 2σ while keeping the prey noise at σ caused tipping times to drop substantially, while the opposite case (where $\sigma_1 = 2\sigma$ and $\sigma_2 = \sigma$) showed essentially no difference. This shows that in environments which are hostile for the predator but survivable for the prey, tipping probability and tipping time are primarily influenced by two separate mechanisms.

Scenario 2. Noise-induced tipping between boundary equilibrium E_K and interior equilibrium E_1^*

When the model parameters are given by $K = 21$, $A = -1$, $a = 0.004905$, $b = -0.10891$, $c = 1$, $d = 24.28$, $m = 1$, and $r = 1$, the deterministic model (2) has bistability between the boundary equilibrium E_K (a stable node) and the interior equilibrium E_1^* (an attracting point). In contrast, the boundary equilibrium E_0 and the interior equilibrium E_2^* are saddles. The vector field of the deterministic model (2) in this scenario is shown in Fig. B.5. Under the disturbance of noise, solutions that should tend to E_1^* in the deterministic model (2) may eventually stabilize in a small neighborhood of E_K (see Fig. B.6(a)), and vice versa (see Fig. B.6(b)).

In this scenario, for most of the values of prey noise σ_1 and predator noise σ_2 that we tested, some similar patterns to those seen in Scenario 1 emerged. However, here it was the predator noise (instead of the prey noise) that primarily determined tipping probability. When the predator population experienced some degree of noise, increasing σ_2 caused a monotonic rise in the probability of tipping from the basin of attraction of the coexistence equilibrium E_1^* to that of the prey-only equilibrium E_K, with this probability eventually reaching 1 (see Fig. 3(a)), and a concave response for the probability of tipping in the other direction that eventually reached zero (see Fig. 3(b)). This mirrored the relationships between noise level and tipping probability from E_K to E_0 and vice versa in Scenario 1: noise caused the probability of tipping to an extinction equilibrium to approach 1, and the probability of tipping to the "better" equilibrium to increase and subsequently return to zero. When the system exhibited both predator noise and prey noise, increasing the ratio of σ_1 to σ_2 lowered the probability of tipping from E_1^*'s basin of attraction to that of E_K and raised the tipping probability from E_K to E_1^*, while decreasing this ratio had the opposite effect. This meant that while the prey noise had lesser impact in determining tipping probability, increasing its magnitude improved the odds of the predator's survival (by pulling solution trajectories towards E_1^* rather than E_K); this state of affairs represents the converse of the results for Scenario 1. When only the prey population had noise, increasing σ_1 caused the probability of tipping from E_K's basin of attraction to that of E_1^* rose to 1, showing opposite trends at high noise levels to the cases where the predator population also exhibited noise. However, solutions starting in the basin of attraction of E_1^* that only experienced prey noise were generally unchanged from their deterministic trajectories

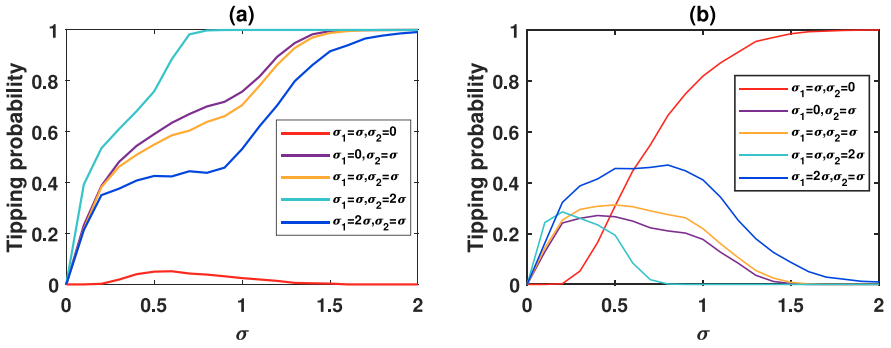

Fig. 3. Tipping probabilities of solution trajectories of the stochastic system (3) with $K = 21, A = -1, a = 0.004905, b = -0.10891, c = 1, d = 24.28, m = 1, r = 1$. The initial values in Figs. 3(a) and 3(b) are given by $(x(0), y(0)) = (0.5, 20)$ and $(x(0), y(0)) = (0.4, 20)$, respectively, within the basins of attraction of the coexistence and prey-only steady states.

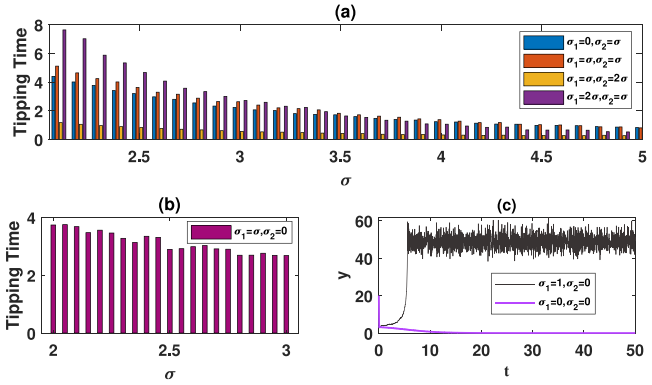

Fig. 4. Tipping times of solution trajectories of the stochastic system (3) with $K = 21, A = -1, a = 0.004905, b = -0.10891, c = 1, d = 24.28, m = 1, r = 1$. The initial values in Figs. 3(a) and 3(b) are given by $(x(0), y(0)) = (0.5, 20)$ and $(x(0), y(0)) = (0.4, 20)$, respectively. Fig. 3(c) is the time series plot of the stochastic model (3) and the corresponding deterministic case (2).

(although a concave relationship between prey-only noise level and tipping probability was observed).

For solutions starting from the basin of attraction of E_1^*, tipping may occur with probability 1 if there is enough noise in the predator population. In this case, if the prey noise intensity is fixed, then the tipping time is negatively correlated with the noise intensity in the predator population, while if the predator noise intensity is fixed, then the tipping time is positively correlated with the noise intensity in the prey population. Tipping time decreases if noise intensities in both predator and prey populations increase simultaneously, suggesting that noise from the predator population plays a dominant role in determining tipping time, as it does for tipping probability in this scenario. Moreover, as noise intensity increases, this decrease happens at a slower rate (see Fig. 4(a)).

Intuitively, since the boundary equilibrium E_K is an absorbing state, the probability of tipping from the boundary equilibrium E_K to the coexistence equilibrium E_1^* is unlikely to reach 1. However, such a transition was observed to occur with probability 1 when the prey population experienced large amounts of noise and the predators experienced none (see Fig. 3(b)). In this case, the tipping time decreases monotonically with increasing noise intensity (see Fig. 4(b)). This suggests that under conditions similar to those in Scenario 2 (e.g. an environment that the prey is very well adapted to), noise within the prey population may be beneficial for population coexistence (see Fig. 4(c)).

Scenario 3. Noise-induced tipping between boundary equilibria E_0, E_K and interior equilibrium E_1^*

Numerical simulation of the deterministic model (2) with parameter values $K = 21$, $A = 1$, $a = 0.004905$, $b = -0.10891$, $c = 1$, $d = 24.28$, $m = 1$, $r = 1$ shows that the boundary equilibria E_0 and E_K are stable nodes, the interior equilibrium E_1^* is an attracting point, and the interior equilibrium E_2^* and the Allee equilibrium E_A are both saddles (see Fig. B.7), which is consistent with the results of Lemma 2.1.

When noise is involved, a solution starting from the basin of attraction of a particular steady state may always fluctuate around that one, or it may pass a critical point and stabilize within the small neighborhood of alternative steady states (see Fig. B.8). The solution may experience multiple wanderings between steady states before it finally settles into the small neighborhood of one of them (e.g., Figs. B.8(b_4) and (c_5)). However, trajectories that approached the zero steady-state tended to stay near it, without fluctuations. We therefore conjecture that the zero steady state may draw in solutions fluctuating around other steady states in finite time, making it potentially the only absorbing state. To further elucidate the relationship between noise intensity and tipping probability of the stochastic system (3), we performed repeated numerical experiments on the state of the stochastic solution when the time is sufficiently large (see Fig. 5). These results are summarized in Table 3. As in Scenario 1, the probability of tipping away from E_0 never reached 1. Additionally, the probability of tipping from a given equilibrium to one that was more conducive to survival (E_0 to either E_K or E_1^*, and E_K to E_1^*) usually followed the concave pattern shown previously.

For solutions starting from the basin of attraction of E_K, there were two cases in which the tipping phenomenon occurs with probability 1, namely when noise is present solely in the prey population and when it is present in both species. In each of these cases, increasing the noise intensity decreases the expected tipping time, although this is a shallow decrease when just the prey is exposed to noise and a steeper one when both species are. Hence, for solutions tipping away from E_K, moderately high noise intensity meant tipping happened more quickly when only the prey suffered from noise, while very high noise intensity meant tipping was faster when both populations suffered from noise (Fig. 6(a)). In cases where the solution starts from the basin of attraction of E_1^* and tipping is assured, tipping time is negatively correlated with noise intensity, especially when noise is present in the predator population. For solutions tipping away from E_1^*, tipping occurs more quickly when the predator is exposed to noise compared to when the prey is, and most quickly when both populations experience noise (Fig. 6(b)).

Scenario 4. Noise-induced tipping between boundary equilibrium E_0, interior equilibrium E_1^* and the stable cycle

When $K = 20$, $A = 2$, $a = 0.004905$, $b = -0.10891$, $c = 1$, $d = 24.28$, $m = 1$, and $r = 1$, the deterministic model (2) admits a periodic cycle. It follows from Fig. B.9 that the boundary equilibrium E_K is a saddle, the boundary equilibrium E_0 is a stable node, and the interior equilibrium E_1^* is an attracting point. In addition, there is a stable cycle around the interior equilibrium E_1^*. Fig. B.10 illustrates how tipping can occur between any combination of the basins of attraction of E_0, E_1^*, and the stable cycle when noise is introduced to the system.

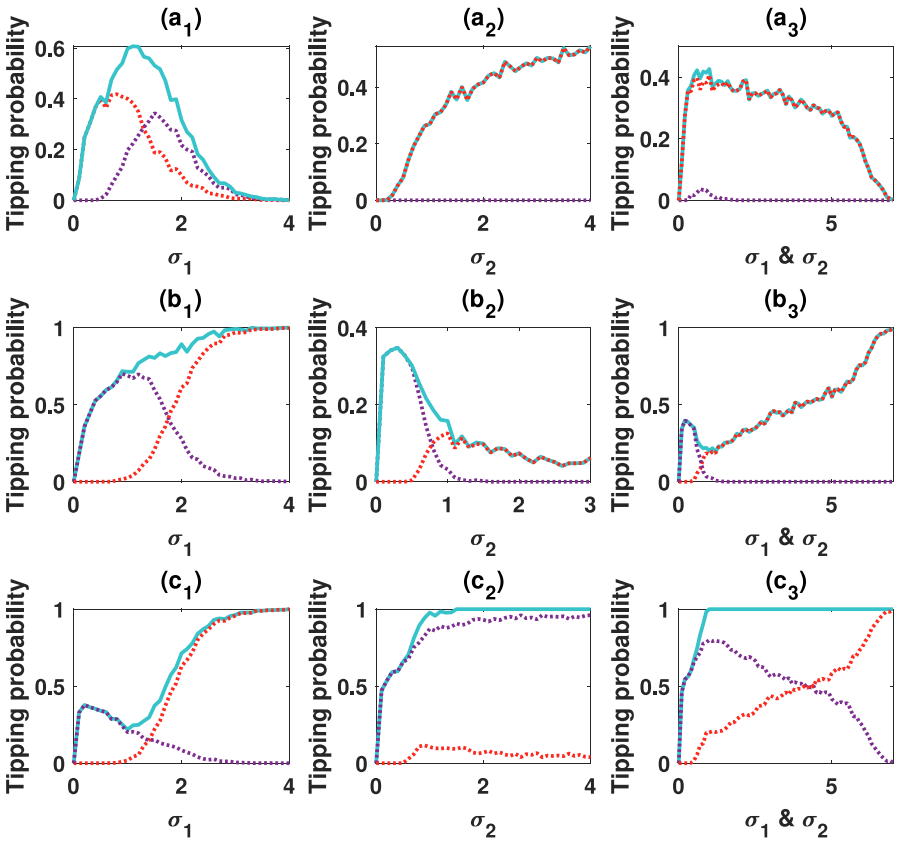

Fig. 5. Tipping probabilities of the stochastic system (3) with $K = 21, A = 1, a = 0.004905, b = -0.10891, c = 1, d = 24.28, m = 1$, and $r = 1$. The initial values in Figs. 5(a_1)-(a_3), 5(b_1)-(b_3), and 5(c_1)-(c_3) are given by $(x(0), y(0)) = (1.3, 11)$, $(1.78, 11)$ and $(1.8, 11)$, respectively. These points lie in the basins of attraction of E_0, E_K, and E_1^*, in that order. In each subfigure, the red and purple lines represent the probability that the solution enters the vicinity of a specific alternative equilibrium; respectively, these are E_K and E_1^* in Fig. 5(a_1)-(a_3), E_0 and E_1^* in Fig. 5(b_1)-(b_3), and E_0 and E_K in Fig. 5(c_1)-(c_3). The green line in each subfigure represents the total probability of tipping.

Table 3
Relationship between noise and tipping probability in the stochastic system (3), organized by which species experiences noise ($\sigma_1 \neq 0$ for the prey, $\sigma_2 \neq 0$ for the predator), which basin of attraction a solution starts in (that of E_0, E_K, or E_1^*), and which steady state the solution tips towards. The option Concave (resp. Positive) means that the relationship between noise intensity and the probability of the solution passing a tipping point and entering a small neighborhood of the specified final steady state (i.e., E_0, E_K, E_1^*) is concave (resp. positive).

Noise source	Initial state	Final state			Total tipping probability
		E_0	E_K	E_1^*	
$\sigma_1 \neq 0, \sigma_2 = 0$	E_0	–	Concave	Concave	Concave
	E_K	Positive	–	Concave	Positive
	E_1^*	Positive	Concave	–	See Fig. 5(c_1)
$\sigma_1 = 0, \sigma_2 \neq 0$	E_0	–	Positive	Irrelevant	Positive
	E_K	Concave	–	Concave	Concave
	E_1^*	Concave	Positive	–	Positive
$\sigma_1 \neq 0, \sigma_2 \neq 0$	E_0	–	Concave	Irrelevant	Concave
	E_K	Positive	–	Concave	See Fig. 5(b_3)
	E_1^*	Positive	Concave	–	Positive

Here, the probability of a solution tipping out of the basin of attraction of E_0 (into those of either E_1^* or the stable cycle) followed patterns that were similar to but more complex than those demonstrated in the other scenarios (Fig. 7(a)). If only the prey was affected by noise, a concave relationship between noise intensity and tipping probability was seen, with the peak probabilities occurring at relatively low values of σ_1. When noise was only experienced by the predator population, the probability of tipping away from the extinction equilibrium E_0 rose with noise intensity in a saturation-like response (after first undergoing a small rise at low intensity). These patterns were akin to those found in Scenarios 1 and 3, the other two that we considered in which E_0 existed. However, we saw here that when both σ_1 and σ_2 were nonzero, complex relationships between noise intensity and tipping probability emerged that resembled hybrids of the cases where only one of the two was present. This stands in contrast to the other scenarios, in which the effects of one noise term (i.e. either σ_1 or σ_2) would dominate those of the other when both were nonzero. In particular, when both the predator and prey experienced noise, the probability of tipping away from E_0 showed a double-concave response to noise intensity, with one peak at low intensity values and another, usually wider, peak at intermediate ones. Increasing the ratio of σ_1 to σ_2 diminished the second peak in tipping probability, thus making the graph of tipping probability as a function of noise intensity more closely resemble the one in the case where $\sigma_2 = 0$. Decreasing that ratio, i.e. making the predator population relatively noisier than the prey, often raised the likelihood of tipping away from E_0, but did not change the fact that

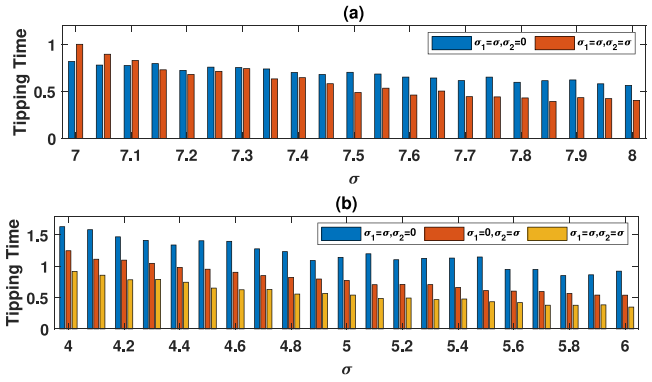

Fig. 6. Tipping times of solution trajectories of the stochastic system (3) with $K = 21, A = 1, a = 0.004905, b = -0.10891, c = 1, d = 24.28, m = 1, r = 1$. The initial values in Figs. 6(a) and 6(b) are given by $(x(0), y(0)) = (1.78, 11)$ and $(x(0), y(0)) = (1.8, 11)$, respectively.

all solution trajectories that started within E_0's attraction basin stayed there for sufficiently large noise magnitudes.

For both E_1^* and the stable cycle, the graphs of the probability of tipping to the extinction equilibrium E_0 as a function of noise intensity (Figs. 7(b) and 7(c)) resembled mirror images of the graph of the probability of tipping away from E_0 when reflected vertically. If noise was present in the prey population, the probability of tipping towards E_0 from either E_1^* or the stable cycle reached 1 for sufficiently large values of noise intensity, with decreases to probabilities less than 1 observed seen for very low and intermediate such values. As mentioned above, this double-dip structure was analogous to the double-concave structure seen in the probabilities of tipping away from E_0. In fact, for all noise configurations and nearly all values of noise intensity that we considered, the sum of the probability of tipping away from E_0 and the probability of tipping from E_1^* to E_0 was very close to 1. (In other words, the concavities in both Figs. 7(a) and 7(b) were of the same size and occurred at the same values of σ.) The probability of tipping from the stable cycle to E_0 followed similar patterns as that of tipping from E_1^* to E_0. However, so long as there was some noise in the predator population, extinction was less probable for solutions starting near the stable cycle than it was for solutions starting in the basin of attraction of E_1^*.

In the cases in this scenario for which tipping to E_0 was assured, extinction time could be decreased by greater noise in the predator population, which was similar to the effects seen in the other scenarios. In particular, if σ_2 (the predator noise) was equal to or larger than σ_1, increasing the noise intensity overall caused solution trajectories that tipped towards E_0 with probability 1 to do so more quickly (Fig. 8). However, if σ_1 was larger than σ_2, noise intensity had very little effect on tipping time.

3.2. Safe areas and extinction warnings

In the previous subsection, we determine tipping probabilities and tipping times of the stochastic system (3) for initial population values close to attraction basin boundaries. To identify how different levels of environmental noise can affect tipping away from these boundaries, we obtain probabilities of tipping to an extinction equilibrium for a wide range of initial conditions for both predator and prey species. Following this, we assign different extinction warnings to these initial population levels according to the extinction probability of predator and prey populations (see Table 4). We assign an initial population density a Level IV (blue) warning when the extinction probability of predator and prey populations is below 20%, at which point the risk of population extinction is relatively low. When the extinction probability of predator and prey populations is between 20% and 50% when starting from a given initial density, we assign that initial condition a Level III (yellow) warning, indicating moderate extinction risk. If an initial condition yields extinction probability of predator and prey populations between 50% and 80%, we assign it a Level II (orange) warning, denoting a high probability of extinction. At extinction probability greater than 80%, an initial population density receives a Level I (red) warning, meaning that the extinction risk of a population starting from that density is extremely high.

Table 4
Warning levels and associated extinction probabilities.

Warning level	Extinction probability	Marker color
Level I warning (Red warning)	≥80%	Red
Level II warning (Orange warning)	50%–80%	Orange
Level III warning (Yellow warning)	20%–50%	Yellow
Level IV warning (Blue warning)	≤20%	Blue

From Section 3.1, we know that in Scenario 2, the deterministic model (2) has bistability between the coexistence equilibrium E_1^* and the prey-only equilibrium E_K, and the basin of attraction is divided into two regions (see Fig. 9(a)). In the deterministic case, we mark the basins of attraction of E_K and E_1^* in red and blue, respectively, which correspond to warning levels I and IV. The green line indicates the boundary of the deterministic basin of attraction for the extinction (in this case prey-only) and coexistence states.

When evaluating warning levels for Scenario 2, we found that the patterns that we saw in tipping probability also manifested themselves in the safety of initial conditions. We found that compared to the baseline case with no noise, introducing noise into the prey population downgraded the warning level for initial conditions with Level I warnings to Level II, Level III, or even Level IV (the lowest risk of extinction; see Fig. 9(b)). This is in concordance with the higher tipping probability from E_K to E_1^* rather than from E_1^* to E_K when $\sigma_1 = 1$ and $\sigma_2 = 0$ (Fig. 3), as well as the fact that increasing σ_1 relative to σ_2 delays tipping in this scenario (Fig. 4). In contrast, when the predator population experienced noise, areas in which the predators would survive in the deterministic case instead saw their warning levels increase (Figs. 9(c)–(f)). When both predator and prey populations were exposed to noise, the different warning areas were hardly distinguishable from the case where only the predator is exposed to noise (Figs. 9(c) and 9(d)), analogous with how predator noise was seen to dominate prey noise in terms of influence on tipping probability in this scenario. Increasing the ratio of σ_1 to σ_2, by taking $\sigma_1 = 2$ and $\sigma_2 = 1$, did not add many initial conditions to the Level IV warning area, but it did shrink the Level I warning area substantially (Fig. 9(e)). This resulted in many initial conditions falling into the two intermediate warning levels, including both initial conditions where the predators deterministically survived and those where they deterministically went extinct. However, decreasing the ratio of σ_1 to σ_2 (by taking $\sigma_1 = 2$ and $\sigma_2 = 1$) enlarged the Level I warning area to encompass all initial conditions for which the starting prey population was less than about 50 (Fig. 9(f)). This meant that the boundary between very high and very low risks of predator extinction now depended solely on the initial prey value. Across all cases, the closer to the deterministic attraction basin boundary an initial condition was, the more significant its change in warning level was; this was consistent with our intuition.

In Scenario 3, the deterministic model (2) is tristable between the extinction states E_0 and E_K and the coexistence state E_1^*. Since we assign warning levels according to the probability of extinction of at least one species, we group the basins of attraction of E_0 and E_K together in this analysis; this combined basin for the deterministic case of the model is marked in red in Fig. 10(a). Likewise, the deterministic basin of attraction of E_1^* is marked in blue. In this scenario, small to moderate amounts of noise in either the predator or prey population had the effect of making the attraction basin boundary less sharp, with Level I warnings near the boundary downgraded to Level II, and

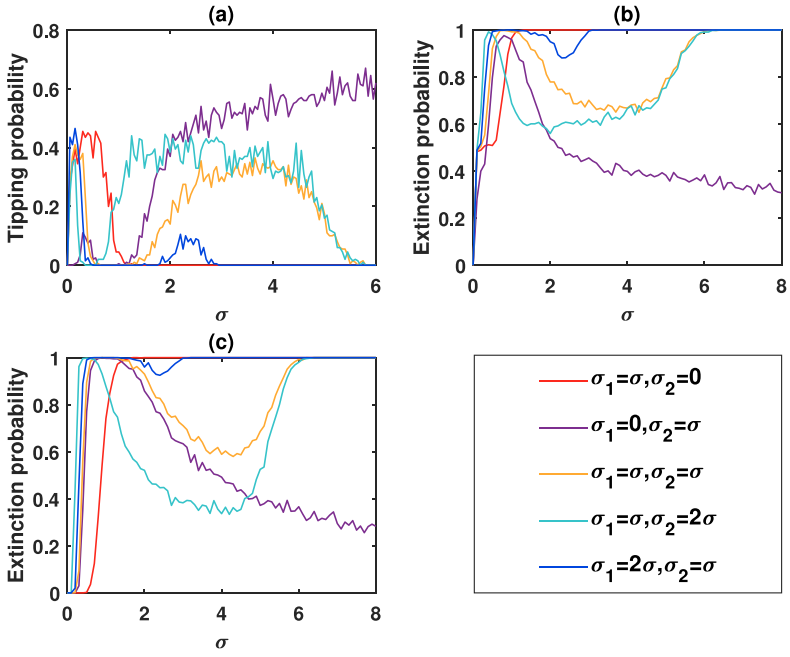

Fig. 7. Tipping probabilities for the stochastic system (3) with $K = 20, A = 2, a = 0.004905, b = -0.10891, c = 1, d = 24.28, m = 1, r = 1$. The initial values in Figs. 7(a), 7(b), and 7(c) are $(x(0), y(0)) = (2.22, 5)$, $(2.23, 5)$ and $(9.8, 32.1)$, respectively, which are in the basins of attraction of E_0, E_1^*, and the stable cycle, respectively. Fig. 7(a) shows the probability of tipping away from E_0 into the basin of attraction of either E_1^* or the stable cycle, while the other two subfigures show the probability of tipping to E_0.

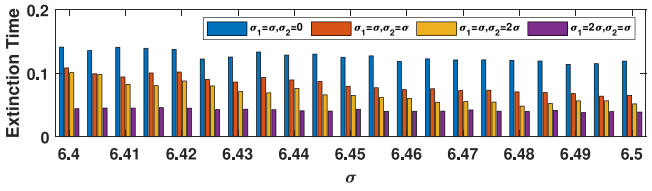

Fig. 8. Extinction times of solution trajectories of the stochastic system (3) with $K = 20, A = 2, a = 0.004905, b = -0.10891, c = 1, d = 24.28, m = 1, r = 1$ and $(x(0), y(0)) = (9.8, 32.1)$.

Level IV warnings upgraded to Level II (see Figs. 10(b)–(d)). This took place as long as the maximum noise value in either was at most 0.5, and stands in contrast to the trends seen in Scenario 2, where the attraction basin boundary could be "moved" in one direction or another depending on which species experienced noise. However, in Scenario 3, further increasing noise levels in either population resulted in the level IV warning area drastically shrinking or even disappearing. Taking $\sigma_1 = 1$ and $\sigma_2 = 0.5$ caused nearly all of the initial conditions that converged to the coexistence equilibrium in the deterministic case to fall under Level III or Level II warnings (Fig. 10(e)), while taking $\sigma_1 = 0.5$ and $\sigma_2 = 1$ led to all initial conditions that we tested being assigned a Level I warning, the most severe (Fig. 10(f)).

In Scenario 4, the deterministic model (2) is tristable between the extinction state (E_0) and two coexistence states (E_1^* and the stable cycle). In this case, the changes in warning levels induced by noise are very similar to those in Scenario 3 (see Fig. 11). Mild noise intensity increases in either population meant that the attraction basin boundary stayed roughly in the same place, but became fuzzier, while more substantial increases (especially in predator noise) facilitated harsher warning levels for initial conditions that would deterministically lead to coexistence.

4. Discussion

Ecosystems can undergo irreversible transitions from one steady-state to another alternative steady-state [5,7]. Environmental stochasticity is recognized as an essential underlying factor leading to such steady-state transitions [20,25]. Within this paper, we first analytically demonstrate the biological plausibility of our stochastic predator–prey model (see Appendix A). Subsequently, we use numerical simulations to evaluate the specific effects of noise intensity and noise type on the probability of, and expected time until, tipping to an alternative steady state. We also rank initial population levels of predators and prey according to the extinction probability of one or more of these populations, providing different extinction warning tiers. This work thus provides an in-depth analysis of the impact of environmental stochasticity on the transition of a predator–prey system with Allee effects and Holling type IV functional response between multiple steady states, based on the modeling framework of stochastic differential equations. An important contribution of this study is to provide a new method for exploring the relationship between environmental stochasticity and tipping points in population systems, and to extend the work of Arsie et al. [76] on the deterministic predator–prey system (2). The methods presented in this work can also be applied to study related problems involving tipping phenomena in other natural systems, such as those representing infectious disease transmission [82–84] and social insect collective behavior [85–87].

Our insights suggest that the effects of noise on tipping-related phenomena are diverse, depending on both the type and intensity of noise and the specific context of the predator–prey system. In our results, noise may be either beneficial or detrimental to population survival, which coincides with the point of view of Petrovskii et al. [88]. One trend that we observed was that the probability of tipping towards a steady state in which more species were viable (e.g. from E_K to E_1^*, from E_0 to E_K or E_1^*) tended to be a concave function of noise intensity, while the probability of tipping to a steady state in which fewer species were viable instead usually monotonically increased with noise intensity. This trend specifically took place so long as the species at risk of extinction suffered from noise: for example, in Scenario 2, the stable equilibria being E_1^* and E_K implied that the predators were at risk of extinction, and the above trend was observed when σ_2 (noise in the predator population) was nonzero. Similarly, we found that in the impact on tipping probability of noise in the population at risk of extinction generally dominated that of noise in the other

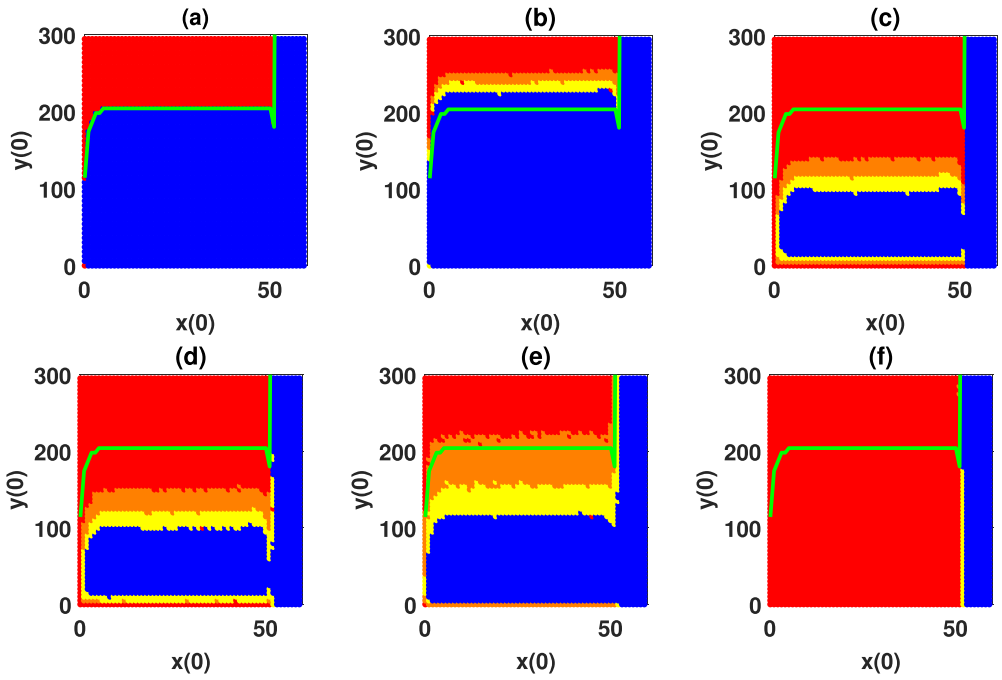

Fig. 9. Warning level of the stochastic system (3) with $K = 21, A = -1, a = 0.004905, b = -0.10891, c = 1, d = 24.28, m = 1, r = 1$. In Fig. 9(a), the noise densities are given by $\sigma_1 = \sigma_2 = 0$. Therefore, the blue and red regions represent the basins of attraction for the coexistence equilibrium (E_1^*) and prey-only equilibrium (E_K), respectively. The green line is the attraction basin boundary. In Figs. 9(b)–(f), the noise densities (σ_1, σ_2) are given by $(1,0)$, $(0,1)$, $(1,1)$, $(2,1)$ and $(1,2)$, respectively. The blue, yellow, orange and red areas indicate the probability of predator extinction as $0\% - 20\%$, $20\% - 50\%$, $50\% - 80\%$ and $80\% - 100\%$, respectively.

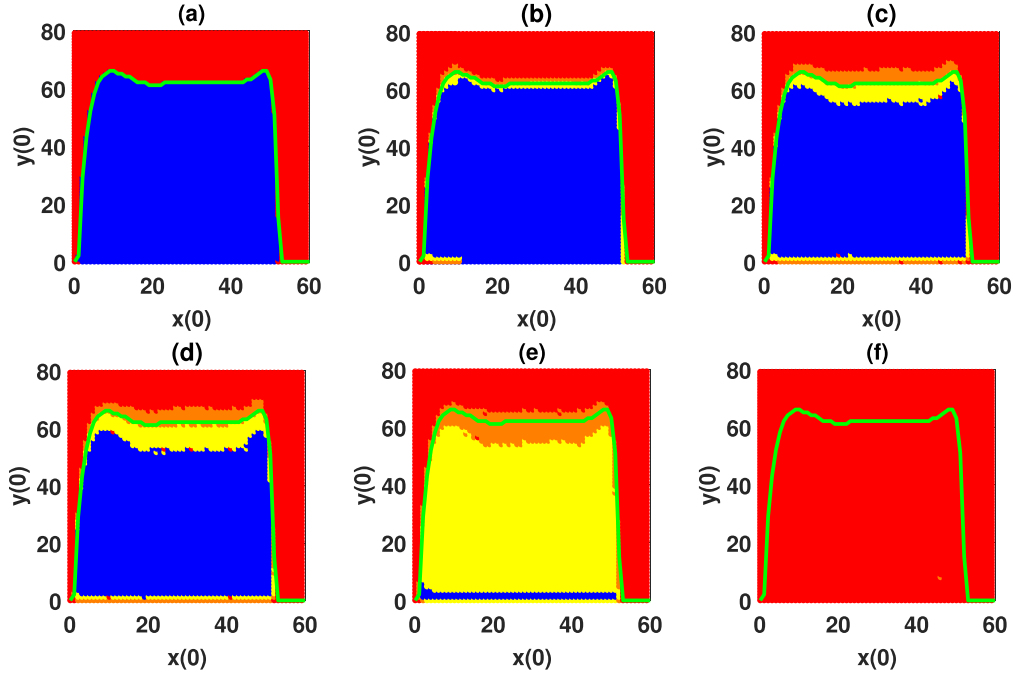

Fig. 10. Warning level of the stochastic system (3) with $K = 21, A = 1, a = 0.004905, b = -0.10891, c = 1, d = 24.28, m = 1, r = 1$. In Fig. 10(a), the noise densities are given by $\sigma_1 = \sigma_2 = 0$. Therefore, the blue and red regions represent the basins of attraction for the coexistence equilibrium (E_1^*) and the equilibria for which at least one species goes extinct ($E_0 \& E_K$), respectively. The green line is the attraction basin boundary. In Figs. 10(b)–(f), the noise densities (σ_1, σ_2) are given by $(0.5, 0)$, $(0, 0.5)$, $(0.5, 0.5)$, $(1, 0.5)$ and $(0.5, 1)$, respectively. The blue, yellow, orange and red areas indicate the probability of simultaneous extinction of predator and prey populations as $0\% - 20\%$, $20\% - 50\%$, $50\% - 80\%$ and $80\% - 100\%$, respectively.

population. (These trends did not show up as much in Scenario 4, since the stable states in that scenario either had both species coexisting or both extinct.) Additionally, the primary determinants of tipping time in all four scenarios were σ_2 and the ratio between σ_1 and σ_2. Increasing the predator noise hastened extinction; increasing the prey noise σ_1 often delayed extinction or offset the effects of σ_2. Furthermore, in both Scenarios 2 and 3, the "worst" steady state with the fewest viable species was observed to be absorbing.

With regards to the tipping warnings for initial conditions that we obtained, our results show that noise intensity may increase or decrease the observed warning level, especially near attraction basin boundaries but also substantially further away from them. In Scenario 2, increases

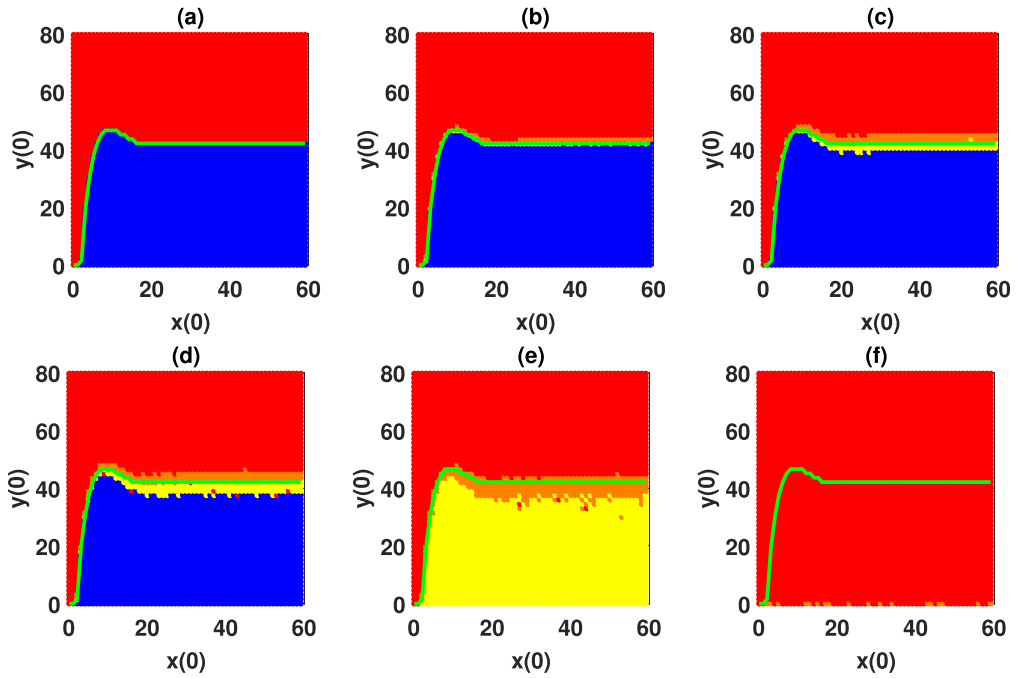

Fig. 11. Warning level of the stochastic system (3) with $K = 20, A = 2, a = 0.004905, b = -0.10891, c = 1, d = 24.28, m = 1, r = 1$. In Fig. 11(a), the noise densities are given by $\sigma_1 = \sigma_2 = 0$. Therefore, the blue and red regions represent the basins of attraction for steady states involving coexistence (E_1^* & the stable cycle) and the extinction equilibrium (E_0), respectively. The green line is the attraction basin boundary. In Figs. 11(b)–(f), the noise densities (σ_1, σ_2) are given by $(0.3, 0)$, $(0, 0.3)$, $(0.3, 0.3)$, $(0.6, 0.3)$ and $(0.3, 0.6)$, respectively. The blue, yellow, orange and red areas indicate the probability of simultaneous extinction of predator and prey populations as $0\% - 20\%$, $20\% - 50\%$, $50\% - 80\%$ and $80\% - 100\%$, respectively.

in predator noise were accompanied by more severe warning levels, while raising prey noise conversely reduced warning levels; this mirrored the pattern found for tipping time in which predator noise was harmful and prey noise was often beneficial for survival. However, in Scenarios 3 and 4, the effect of noise in either population was similar, namely to blur the attraction basin boundary and raise warning levels for initial conditions that would ordinarily result in coexistence. This may stem from the fact that in these scenarios, both species carry at least some risk of extinction (rather than just the predator, as in Scenario 2), so noise in both populations may be expected to have analogous effects. In all three scenarios that we evaluated warning levels for, the effects of predator noise dominated those of prey noise. The diverse insights in our work send us an important message that in species conservation or farming of commercial species, adaptive early warning mechanisms should be developed according to the specific environment in which the species is located in case catastrophic population extinction occurs.

To incorporate environmental stochasticity into the deterministic population system (2) proposed by Arsie et al. [76], this work assumes that the type of environmental stochasticity obeys uncorrelated standard white Gaussian noise whose intensity is positively correlated with the population density. This classical assumption has been widely used in recent years to assess the impact of environmental stochasticity on the dynamics of biological systems [89,90], based on the fact that biological populations are more susceptible to environmental factors such as rainfall and temperature. In some specific scenarios, the population may also suffer from other types of environmental stochasticity such as telegraph noise and Lévy noise [78,91]; for example, rare but potentially catastrophic events within an ecosystem have been described using Lévy noise. The impact on these types of environmental stochasticity is beyond the scope of this work, but will be one of our future research questions.

At the same time, there are some limitations in this work. One of the examined scenarios (specifically Scenario 4) involved tipping into and out of a basin of attraction for a stable cycle. It is of great significance to further analyze which parts of the limit cycle are more prone to tipping, and the proportion of time that the solution spends in these parts. Techniques from the literature on phase tipping will be helpful in this regard. Furthermore, numerical simulations suggest that the extinction equilibrium may be the unique absorbing state of the stochastic predator–prey system (3). New theoretical techniques need to be developed to prove this conjecture.

Declaration of competing interest

The authors declare that they have no known competing financial interests or personal relationships that could have appeared to influence the work reported in this paper.

Acknowledgments

T. Feng's research was partially supported by the National Natural Science Foundation of China (Grant No. 12201548), the Natural Science Foundation of Jiangsu Province, PR China (Grant No. BK20220553) and the Scholarship Foundation of China Scholarship Council (Award Number 202308320279). H. Wang's research was partially supported by the Natural Sciences and Engineering Research Council of Canada (Individual Discovery Grant RGPIN-2020-03911 and Discovery Accelerator Supplement Award RGPAS-2020-00090).

Appendix A. Supplementary data

Supplementary material related to this article can be found online at https://doi.org/10.1016/j.mbs.2023.109075.

References

[1] A. Vanselow, S. Wieczorek, U. Feudel, When very slow is too fast-collapse of a predator-prey system, J. Theoret. Biol. 479 (2019) 64–72.
[2] T.M. Bury, R. Sujith, I. Pavithran, M. Scheffer, T.M. Lenton, M. Anand, C.T. Bauch, Deep learning for early warning signals of tipping points, Proc. Natl. Acad. Sci. 118 (39) (2021) e2106140118.

[3] R.A. Ims, J.-A. Henden, S.T. Killengreen, Collapsing population cycles, Trends Ecol. Evol. 23 (2) (2008) 79–86.
[4] L. Dai, D. Vorselen, K.S. Korolev, J. Gore, Generic indicators for loss of resilience before a tipping point leading to population collapse, Science 336 (6085) (2012) 1175–1177.
[5] J.M. Drake, B.D. Griffen, Early warning signals of extinction in deteriorating environments, Nature 467 (7314) (2010) 456–459.
[6] C. Boettiger, A. Hastings, Early warning signals and the prosecutor's fallacy, Proc. R. Soc. B 279 (1748) (2012) 4734–4739.
[7] A. Hastings, Timescales and the management of ecological systems, Proc. Natl. Acad. Sci. 113 (51) (2016) 14568–14573.
[8] J. Jiang, A. Hastings, Y.-C. Lai, Harnessing tipping points in complex ecological networks, J. R. Soc. Interface 16 (158) (2019) 20190345.
[9] J. Jiang, Z.-G. Huang, T.P. Seager, W. Lin, C. Grebogi, A. Hastings, Y.-C. Lai, Predicting tipping points in mutualistic networks through dimension reduction, Proc. Natl. Acad. Sci. 115 (4) (2018) E639–E647.
[10] J.J. Lever, E.H. van Nes, M. Scheffer, J. Bascompte, The sudden collapse of pollinator communities, Ecol. Lett. 17 (3) (2014) 350–359.
[11] J.M. Tylianakis, C. Coux, Tipping points in ecological networks, Trends Plant Sci. 19 (5) (2014) 281–283.
[12] A.K. Klose, V. Karle, R. Winkelmann, J.F. Donges, Emergence of cascading dynamics in interacting tipping elements of ecology and climate, R. Soc. Open Sci. 7 (6) (2020) 200599.
[13] P.E. O'Keeffe, S. Wieczorek, Tipping phenomena and points of no return in ecosystems: beyond classical bifurcations, SIAM J. Appl. Dyn. Syst. 19 (4) (2020) 2371–2402.
[14] T. Wilkat, T. Rings, K. Lehnertz, No evidence for critical slowing down prior to human epileptic seizures, Chaos 29 (9) (2019) 091104.
[15] P.M. Müller, J. Heitzig, J. Kurths, K. Lüdge, M. Wiedermann, Anticipation-induced social tipping: can the environment be stabilised by social dynamics? Eur. Phys. J. Spec. Top. 230 (16) (2021) 3189–3199.
[16] A. Vanselow, L. Halekotte, U. Feudel, Evolutionary rescue can prevent rate-induced tipping, Theoret. Ecol. 15 (1) (2022) 29–50.
[17] C. Kiers, C.K. Jones, On conditions for rate-induced tipping in multi-dimensional dynamical systems, J. Dynam. Differential Equations 32 (1) (2020) 483–503.
[18] R. Arumugam, V. Chandrasekar, D. Senthilkumar, Rate-induced tipping and regime shifts in a spatial ecological system, Eur. Phys. J. Spec. Top. 230 (16) (2021) 3221–3227.
[19] R. Benzi, A. Sutera, A. Vulpiani, The mechanism of stochastic resonance, J. Phys. A: Math. Gen. 14 (11) (1981) 453–457.
[20] P.D. Ditlevsen, S.J. Johnsen, Tipping points: early warning and wishful thinking, Geophys. Res. Lett. 37 (19) (2010).
[21] A. Mallela, A. Hastings, The role of stochasticity in noise-induced tipping point cascades: a master equation approach, Bull. Math. Biol. 83 (5) (2021) 1–20.
[22] H. Alkhayuon, R.C. Tyson, S. Wieczorek, Phase tipping: how cyclic ecosystems respond to contemporary climate, Proc. R. Soc. Lond. Ser. A Math. Phys. Eng. Sci. 477 (2254) (2021) 20210059.
[23] H.M. Alkhayuon, P. Ashwin, Rate-induced tipping from periodic attractors: Partial tipping and connecting orbits, Chaos 28 (3) (2018) 033608.
[24] R. Lande, S. Engen, B.-E. Saether, et al., Stochastic Population Dynamics in Ecology and Conservation, Oxford University Press on Demand, New York, 2003.
[25] Y. Meng, Y.-C. Lai, C. Grebogi, Tipping point and noise-induced transients in ecological networks, J. R. Soc. Interface 17 (171) (2020) 20200645.
[26] L. Ryashko, Sensitivity analysis of the noise-induced oscillatory multistability in Higgins model of glycolysis, Chaos 28 (3) (2018) 033602.
[27] J. Terborgh, L. Lopez, P. Nuñez, M. Rao, G. Shahabuddin, G. Orihuela, M. Riveros, R. Ascanio, G.H. Adler, T.D. Lambert, L. Balbas, Ecological meltdown in predator-free forest fragments, Science 294 (5548) (2001) 1923–1926.
[28] A. Sinclair, S. Mduma, J.S. Brashares, Patterns of predation in a diverse predator–prey system, Nature 425 (6955) (2003) 288–290.
[29] B. Zhang, L. Zhai, J. Bintz, S.M. Lenhart, W. Valega-Mackenzie, J.D. Van Dyken, The optimal controlling strategy on a dispersing population in a two-patch system: Experimental and theoretical perspectives, J. Theoret. Biol. 528 (2021) 110835.
[30] M. Sieber, F.M. Hilker, The hydra effect in predator–prey models, J. Math. Biol. 64 (1) (2012) 341–360.
[31] A.J. Lotka, Elements of Physical Biology, Williams & Wilkins, Baltimore, Maryland, 1925.
[32] V. Volterra, Variazioni e Fluttuazioni del Numero d'Individui in Specie Animali Conviventi, Memorie del R. Comitato Talassografico Italiano, Men. CXXXI, 1927.
[33] M. Costa, C. Hauzy, N. Loeuille, S. Méléard, Stochastic eco-evolutionary model of a prey-predator community, J. Math. Biol. 72 (3) (2016) 573–622.
[34] P. Panday, N. Pal, S. Samanta, P. Tryjanowski, J. Chattopadhyay, Dynamics of a stage-structured predator-prey model: cost and benefit of fear-induced group defense, J. Theoret. Biol. 528 (2021) 110846.
[35] Y. Tao, J. Ren, The stability and bifurcation of homogeneous diffusive predator–prey systems with spatio–temporal delays, Discrete Contin. Dyn. Syst. Ser. B 27 (1) (2022) 229.
[36] P. Srinivasu, B. Prasad, Role of quantity of additional food to predators as a control in predator–prey systems with relevance to pest management and biological conservation, Bull. Math. Biol. 73 (10) (2011) 2249–2276.
[37] D. Xiao, L.S. Jennings, Bifurcations of a ratio-dependent predator-prey system with constant rate harvesting, SIAM J. Appl. Math. 65 (3) (2005) 737–753.
[38] H. Yokoi, K.-i. Tainaka, K. Sato, Metapopulation model for a prey-predator system: Nonlinear migration due to the finite capacities of patches, J. Theoret. Biol. 477 (2019) 24–35.
[39] B. Spiecker, T.C. Gouhier, F. Guichard, Reciprocal feedbacks between spatial subsidies and reserve networks in coral reef meta-ecosystems, Ecol. Appl. 26 (1) (2016) 264–278.
[40] Y. Tao, S.A. Campbell, F.J. Poulin, Dynamics of a diffusive Nutrient-Phytoplankton-Zooplankton model with spatio-temporal delay, SIAM J. Appl. Math. 81 (6) (2021) 2405–2432.
[41] T. Dondè, Uniform persistence in a prey–predator model with a diseased predator, J. Math. Biol. 80 (4) (2020) 1077–1093.
[42] J.C. Gascoigne, R.N. Lipcius, Allee effects driven by predation, J. Appl. Ecol. 41 (5) (2004) 801–810.
[43] A.M. Kramer, B. Dennis, A.M. Liebhold, J.M. Drake, The evidence for Allee effects, Popul. Ecol. 51 (3) (2009) 341–354.
[44] E. Angulo, G.M. Luque, S.D. Gregory, J.W. Wenzel, C. Bessa-Gomes, L. Berec, F. Courchamp, Allee effects in social species, J. Anim. Ecol. 87 (1) (2018) 47–58.
[45] F. Courchamp, D.W. Macdonald, Crucial importance of pack size in the African wild dog Lycaon pictus, Animal Conserv. 4 (2001) 169–174.
[46] R. Nagel, C. Stainfield, C. Fox-Clarke, C. Toscani, J. Forcada, J.I. Hoffman, Evidence for an Allee effect in a declining fur seal population, Proc. R. Soc. B 288 (1947) (2021) 20202882.
[47] E.E. Hackney, J.B. McGraw, Experimental demonstration of an Allee effect in American ginseng, Conserv. Biol. 15 (1) (2001) 129–136.
[48] H.G. Davis, C.M. Taylor, J.G. Lambrinos, D.R. Strong, Pollen limitation causes an Allee effect in a wind-pollinated invasive grass (Spartina alterniflora), Proc. Natl. Acad. Sci. 101 (38) (2004) 13804–13807.
[49] B. Dennis, Allee effects: population growth, critical density, and the chance of extinction, Nat. Resour. Model. 3 (4) (1989) 481–538.
[50] C. Bessa-Gomes, S. Legendre, J. Clobert, Allee effects, mating systems and the extinction risk in populations with two sexes, Ecol. Lett. 7 (9) (2004) 802–812.
[51] C.M. Taylor, A. Hastings, Allee effects in biological invasions, Ecol. Lett. 8 (8) (2005) 895–908.
[52] F. Courchamp, E. Angulo, P. Rivalan, R.J. Hall, L. Signoret, L. Bull, Y. Meinard, Rarity value and species extinction: the anthropogenic Allee effect, PLoS Biol. 4 (12) (2006) e415.
[53] W.E. Johnson, D.P. Onorato, M.E. Roelke, E.D. Land, M. Cunningham, R.C. Belden, R. McBride, D. Jansen, M. Lotz, D. Shindle, et al., Genetic restoration of the Florida panther, Science 329 (5999) (2010) 1641–1645.
[54] M.T. Alves, F.M. Hilker, Hunting cooperation and Allee effects in predators, J. Theoret. Biol. 419 (2017) 13–22.
[55] M. Fan, P. Wu, Z. Feng, R.K. Swihart, Dynamics of predator–prey metapopulations with Allee effects, Bull. Math. Biol. 78 (8) (2016) 1727–1748.
[56] B.N. McLellan, R. Serrouya, H.U. Wittmer, S. Boutin, Predator-mediated Allee effects in multi-prey systems, Ecology 91 (1) (2010) 286–292.
[57] A.J. Terry, Predator–prey models with component Allee effect for predator reproduction, J. Math. Biol. 71 (6) (2015) 1325–1352.
[58] J. Wang, J. Shi, J. Wei, Predator–prey system with strong Allee effect in prey, J. Math. Biol. 62 (3) (2011) 291–331.
[59] E. González-Olivares, A. Rojas-Palma, Multiple limit cycles in a Gause type predator–prey model with Holling type III functional response and Allee effect on prey, Bull. Math. Biol. 73 (6) (2011) 1378–1397.
[60] H.I. Freedman, G.S. Wolkowicz, Predator-prey systems with group defence: the paradox of enrichment revisited, Bull. Math. Biol. 48 (5–6) (1986) 493–508.
[61] J.B. Collings, The effects of the functional response on the bifurcation behavior of a mite predator–prey interaction model, J. Math. Biol. 36 (2) (1997) 149–168.
[62] J.-c. Huang, D.-m. Xiao, Analyses of bifurcations and stability in a predator-prey system with Holling type-IV functional response, Acta Math. Appl. Sin. 20 (1) (2004) 167–178.
[63] X. Liu, Q. Huang, Analysis of optimal harvesting of a predator-prey model with Holling type IV functional response, Ecol. Complex. 42 (2020) 100816.
[64] T. Caro, Antipredator Defenses in Birds and Mammals, University of Chicago Press, 2005.
[65] E. Líznarová, S. Pekár, Dangerous prey is associated with a type 4 functional response in spiders, Anim. Behav. 85 (6) (2013) 1183–1190.
[66] N. Heuermann, F. van Langevelde, S.E. van Wieren, H.H. Prins, Increased searching and handling effort in tall swards lead to a Type IV functional response in small grazing herbivores, Oecologia 166 (3) (2011) 659–669.
[67] G. Wolkowicz, Bifurcation analysis of a predator-prey system involving group defence, SIAM J. Appl. Math. 48 (3) (1988) 592–606.
[68] D. Xiao, S. Ruan, Global analysis in a predator-prey system with nonmonotonic functional response, SIAM J. Appl. Math. 61 (4) (2001) 1445–1472.
[69] M.C. Köhnke, I. Siekmann, H. Seno, H. Malchow, A type IV functional response with different shapes in a predator–prey model, J. Theoret. Biol. 505 (2020) 110419.
[70] G. Gause, The Struggle for Existence, Williams & Wilkins, Baltimore, Maryland, 1934.

[71] W. Allee, E.S. Bowen, Studies in animal aggregations: mass protection against colloidal silver among goldfishes, J. Exp. Zool. 61 (2) (1932) 185–207.
[72] Y. Fathipour, B. Maleknia, Mite predators, in: Omkar (Ed.), Ecofriendly Pest Management for Food Security, Academic Press, San Diego, 2016, pp. 329–366.
[73] M. Koen-Alonso, P. Yodzis, Dealing with model uncertainty in trophodynamic models: a patagonian example, in: P. de Ruiter, V. Wolters, J.C. Moore, K. Melville-Smith (Eds.), Dynamic Food Webs, in: Theoretical Ecology Series, Vol. 3, Academic Press, Burlington, 2005, pp. 381–394.
[74] C.S. Holling, The components of predation as revealed by a study of small-mammal predation of the European Pine Sawfly1, Canad. Entomol. 91 (5) (1959) 293–320.
[75] C.S. Holling, Principles of insect predation, Ann. Rev. Entomol. 6 (1) (1961) 163–182.
[76] A. Arsie, C. Kottegoda, C. Shan, A predator-prey system with generalized Holling type IV functional response and Allee effects in prey, J. Differential Equations 309 (2022) 704–740.
[77] A. Sau, B. Saha, S. Bhattacharya, An extended stochastic Allee model with harvesting and the risk of extinction of the herring population, J. Theoret. Biol. 503 (2020) 110375.
[78] L. Videla, Strong stochastic persistence of some Lévy-driven Lotka–Volterra systems, J. Math. Biol. 84 (3) (2022) 1–44.
[79] A. Hening, D.H. Nguyen, G. Yin, Stochastic population growth in spatially heterogeneous environments: the density-dependent case, J. Math. Biol. 76 (2018) 697–754.
[80] J.M.T. Thompson, J. Sieber, Predicting climate tipping as a noisy bifurcation: a review, Int. J. Bifurcation Chaos 21 (02) (2011) 399–423.
[81] D.J. Higham, An algorithmic introduction to numerical simulation of stochastic differential equations, SIAM Rev. 43 (3) (2001) 525–546.
[82] C.M. Saad-Roy, N.S. Wingreen, S.A. Levin, B.T. Grenfell, Dynamics in a simple evolutionary-epidemiological model for the evolution of an initial asymptomatic infection stage, Proc. Natl. Acad. Sci. 117 (21) (2020) 11541–11550.
[83] X. Zhang, C. Shan, Z. Jin, H. Zhu, Complex dynamics of epidemic models on adaptive networks, J. Differential Equations 266 (1) (2019) 803–832.
[84] A. Wang, Y. Xiao, R. Smith, Multiple equilibria in a non-smooth epidemic model with medical-resource constraints, Bull. Math. Biol. 81 (4) (2019) 963–994.
[85] Y. Kang, G. Theraulaz, Dynamical models of task organization in social insect colonies, Bull. Math. Biol. 78 (5) (2016) 879–915.
[86] O. Udiani, N. Pinter-Wollman, Y. Kang, Identifying robustness in the regulation of collective foraging of ant colonies using an interaction-based model with backward bifurcation, J. Theoret. Biol. 367 (2015) 61–75.
[87] T. Feng, Z. Qiu, Y. Kang, Recruitment dynamics of social insect colonies, SIAM J. Appl. Math. 81 (4) (2021) 1579–1599.
[88] S.V. Petrovskii, H. Malchow, F.M. Hilker, E. Venturino, Patterns of patchy spread in deterministic and stochastic models of biological invasion and biological control, Biol. Invasions 7 (5) (2005) 771–793.
[89] A. Hening, Y. Li, Stationary distributions of persistent ecological systems, J. Math. Biol. 82 (7) (2021) 1–53.
[90] A. Hening, D.H. Nguyen, P. Chesson, A general theory of coexistence and extinction for stochastic ecological communities, J. Math. Biol. 82 (6) (2021) 1–76.
[91] D. Li, S. Liu, et al., Threshold dynamics and ergodicity of an SIRS epidemic model with semi-Markov switching, J. Differential Equations 266 (7) (2019) 3973–4017.